Study and Design of a Multi-range Programmable Sensor for Temperature Measurements

Khalid Alsnaie
Electrical Engineering Department
College of Engineering
Imam Mohammad Ibn Saud Islamic University
Riyadh, Saudi Arabia
kalsnaie@imamu.edu.sa

Sidi M. Ahmed Ghaly
Electrical Engineering Department
College of Engineering
Imam Mohammad Ibn Saud Islamic University
Riyadh, Saudi Arabia
smghaly@imamu.edu.sa

Md. Asad Ali
Electrical Engineering Department
College of Engineering
Imam Mohammad Ibn Saud Islamic University
Riyadh, Saudi Arabia
asadali@imamu.edu.sa

Received: 6 September 2022 | Revised: 15 September 2022 | Accepted: 17 September 2022

Abstract—In this paper, a wide-range high-precision sensor has been designed in order to accurately measure the temperature in a medium with arbitrary temperature variation and the implementation of a wide-spectrum temperature measurement system with a self-selected multi-sensor has been realized. This multi-sensor core is made up of different sensors combined to measure different temperature ranges. This concept can be used for high-precision temperature measurement in electrical capacitance tomography applications. The proposed technique is well suited for temperatures in boilers, industries, and everywhere high temperature measurement sensitivity is needed by using different combined temperature sensors of high precision.

Keywords-thermocouple; simulation; thermistor; RTD; temperature; linearization; LabVIEW

I. INTRODUCTION

Temperature sensors are among the most widely used sensors in the electronics industry, with applications ranging from safety calibrations to heating, ventilation, and air conditioning (HVAC) in various industries. Despite their widespread use, temperature sensors and their implementation can present challenges for designers to achieve the best performance at the lowest possible cost. There are many ways to detect temperature. The most common methods use temperature sensors like thermistors, resistance temperature sensors, thermocouples, or silicon thermometers. However, choosing the right sensor is only part of the solution because that sensor must be connected to a signal chain that maintains the integrity of the signal, while providing precise compensation for the unique characteristics of the specific sensing technology to ensure an accurate digital temperature representation [1-4].

This article presents a USB-powered circuit solution to perform this task with a multi range system. This solution uses three sensors which are a Negative Temperature Coefficient (NTC) thermistor, a Resistance Temperature Detector (RTD), and a thermocouple to accurately monitor temperature [5-6].

II. IDENTIFICATION OF SENSORS AND THEIR RANGE

RTDs can be constructed in different forms and have good performance in terms of stability, accuracy, and repeatability. The RTD requires a power source to operate and uses an electrical resistance for measurement of temperature. The operation of the RTD sensor is based on the resistance-temperature relationship of the material used in its construction. The amount of change observed in the resistance value of the material due to a temperature rise per degree is measured and the sensor is calibrated accordingly [7-8]. The resistive element is fragile and always requires insulation, so insulator wires are attached to the element. For temperatures below 250°C, insulators such as silicon rubber and PVC are used for this purpose. A metal alloy chemically inert at this temperature is used as a protective sheath to house the measurement point and the leads.

A. RTD Wiring Configurations

RTDs come with two-lead, three-lead, or four-lead wires per element. A two-wire RTD is the least expensive, but the lead wire resistance unavoidably affects the measurement results. Two-wire RTDs are mostly used with short lead wires or where high accuracy is not required. The advantage of the three-wire RTD is that it removes the lead wire resistance from the measurement by adding a third lead wire. Four-wire RTD are used where superior accuracy is critical [5]. The Callendar-Van Dusen equation is commonly used to approximate the RTD curve [9]. Equation (1) is used for $-200 < °C < 0$ and (2) for $0 < °C < 850$.

$$R_T = R_0[1 + AT + BT^2 + CT^3(T - 100)] \quad (1)$$

$$R_T = R_0[1 + AT + BT^2] \quad (2)$$

where R_T is the resistance of the wire at temperature T°C, R_0 is the resistance of the wire at temperature 0°C, A, B, and C are constants used to scale the RTD, with $A = 3.9083 \times 10^{-3} °C^{-1}$, $B = -5.775 \times 10^{-7} °C^{-2}$, and $C = -4.183 \times 10^{-12} °C^{-3}$.

Corresponding author: Khalid Alsnaie

The temperature coefficient α = 0.00385C^{-1} for a platinum wire RTD is given by:

$$a(\Omega/\Omega/^{o}\,\mathrm{C}) = (R_{100} - R_0)/R_0 \times 100^{o}\,\mathrm{C}) \quad (3)$$

B. Wheatstone Bridge Measurement Circuit

Wheatstone bridge circuits are used in sensor circuits. The bridges can be symmetric or asymmetric, balanced or unbalanced. Wheatstone bridge circuits can be used to accurately measure unknown impedance. The Wheatstone bridge has a single impedance-variable element that is inherently nonlinear, away from the balance point. Bridge circuits are commonly used to detect the temperature of a boiler or a process situated away from the actual circuit. Usually a sensor element, typically an RTD situated in the hot/cold environment provides the information about resistance change to calculate temperature [10]. Resistance-variable Wheatstone bridge circuits perform most of the front-end tasks in a design that uses inexpensive and accurate discrete parts. By incorporating an RTD element, the bridge's inherent resistance variations are kept within the accepted linearity and tolerance limits, depending on the manufacturer of the RTD [10].

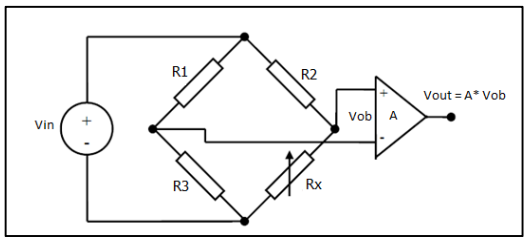

Fig. 1. Wheatstone bridge circuit.

C. Linearization of the Output Bridge

The feedback compensation scheme is used to linearize the output of the bridge. The proposed scheme is shown in Figure 2, which is used with an RTD. The output of the bridge Vop is amplified by an instrumentation amplifier of gain A to obtain the final output Vout. A part of the output is added to a reference voltage VR, employing a unity gain adder and the output of the adder provides the bridge excitation V_B.

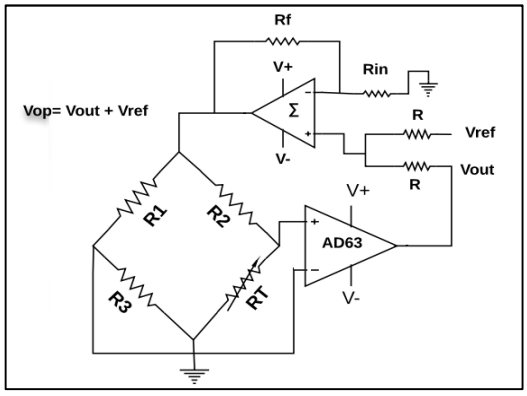

Fig. 2. Feedback compensation scheme with RTD R_T.

$$V_{op} = \left(+\frac{R_f}{R_{in}}\right)\left(\frac{V_{out}+V_{ref}}{2}\right) \quad (4)$$

$$V_{op} = \left(V_{out} + V_{ref}\right) \quad (5)$$

where $R_f = R_{in}$, R_f is the feedback resistor, R_{in} is the input resistor of the OPAMP, V_{out} is the the output voltage of the bridge, V_{ref} is the reference voltage, and V_{op} the summing voltage of the OPAMP

D. Thermistors

A thermistor is a temperature sensing element made of sintered semiconductor material that is characterized by large variations in resistance proportional to small changes in temperature. Thermistors generally have Negative Temperature Coefficients (NTC thermistors), which means that the resistance of the thermistor decreases as the temperature increases [5]. Thermistors are made from a combination of metals and metal oxide materials. Once combined, the materials are formed and fired into the desired shape. The thermistors can then be used as disc-shaped thermistors or can be formed and assembled with lead wires and coatings to form bead-shaped thermistors.

E. Characteristics of an NTC Thermistor

A thermistor is a temperature-sensitive resistor available in two forms: the Positive Temperature Coefficient (PTC) thermistor and the NTC thermistor. The polycrystalline ceramic PTC thermistor has a high PTC and is generally used in switching applications. The NTC ceramic semiconductor thermistor has a high resistive NTC, which causes its resistance to decrease as the temperature increases. This feature makes it a suitable device for precision temperature measurement. An NTC thermistor has 3 modes of operation: resistance versus temperature, voltage versus current, and current versus time. The mode that exploits the characteristics of resistance versus temperature provides the most accurate results. The circuits of the resistance versus temperature mode configure the thermistor in a "zero power" condition. The zero-power condition assumes that the current or voltage excitation of the device does not cause the thermistor to self-heat. The resistor formula of the thermistor is:

$$R_{th} = R_0 \exp[\beta(\frac{1}{T} - \frac{1}{T_0})] \quad (6)$$

where R_{th} is the resistance at temperature T°C, R_0 the resistance at temperature 25°C, β is the temperature constant, T is the temperature of thermistor, and T_0 the temperature at 25°C.

Equation (6) shows the high degree of nonlinearity of the 4.7KΩ thermistor. The rate at which the resistance of an NTC thermistor decreases with temperature is the constant β. Correction of the non-linear response of the thermistor can be done using a simpler and less expensive hardware technique which, when applied, keeps the linearization problem of the thermistor under control for a range of temperatures of ±25°C. A simple approach to first-level linearization of the thermistor output is to place the thermistor in parallel with a standard (1%, metal-film) resistor and a voltage source. The value of the parallel resistance determines the median of the linear region of the thermistor circuit. The resistance value of the thermistor

(R_T) and the Steinhart-Hart equation determine the temperature of the thermistor (Figure 3). The Steinhart-Hart equation has proven to be the best mathematical expression for determining the temperature of an NTC thermistor. The equation of the output voltage with linear thermistor is:

$$V_{out} = V_{in}(\frac{R_T R_2}{R_T + R_2 + R_1 + R_1(R_2 + R} \quad (7)$$

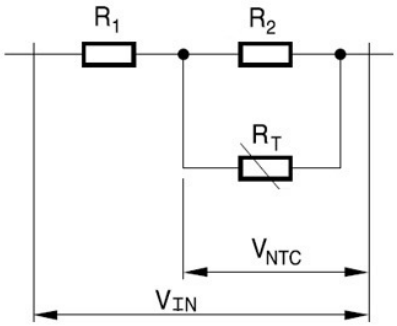

Fig. 3. Thermistor circuit with thermistor R_T.

F. Thermocouple

The operating principle of thermocouples is essentially based on the Seebeck effect. When a temperature difference occurs along a wire, charge transfer occurs. The amount of charge transfer depends on the electrical characteristics of the chosen material. When two wires of different materials are soldered on one side and a temperature difference occurs, a voltage is formed at both free ends. This voltage depends on the temperature difference along the two junctions. To measure the temperature at the junction point, the temperature at the free end must be known. When the free end temperature is unknown, the end must be extended with a compensation cable to a known temperature zone (compensation point) [11]. The compensation point temperature must be known and constant.

G. Thermocouple Linearization Techniques

A novel circuit for linearization of thermocouple signals using Analog – to – Digital (ADC) converter is proposed. The present method utilizes the ratio metric property of ADCs and the converter performs analog to digital conversion as well as linearization. The resulting circuit also has provision for scaling the linearized digital output to obtain a desired full-scale value. The digital count output L of dual-slope integration type A/D converter with differential input is given by:

$$L = \frac{C(V_{in}^{+} - V_{in}^{-})}{V} \quad (8)$$

where V^+ in and V^- in are the analog input voltages, V_{ref} an analog reference voltage, and C is the digital count output when $[(V^+_{in}) - (V^-_{in})]$

If V^+ in the voltage signal $E(x)$ from a transducer circuit (x being measured), following an approach proposed by Ayman A. Ali –a linear relation between $L(x)$ and x can be achieved by suitably modifying (8) such that:

$$L(x) = \frac{C(1+K)E(x)/E_r}{1+KE(x)/E_r} \quad (9)$$

where the analog reference voltage is:

$$VRef(x) = \frac{E_r + KE(x)}{1+K} \text{ for positive } K$$

$$VRef(x) = E_r + KE(x) \text{ for negative } K \quad (10)$$

where K is a linearizing coefficient, whose optimum value is to be determined. The linearizing coefficient in terms of circuit resistances is $K=R_2/R_1$, where x is the temperature T under measurement and $E(x)$ is $E(T)$ - the thermo-e.m.f. from the thermocouple after appropriate reference junction compensation.

As an alternate approach, the linearizing arrangement is designed so that the scaling and linearizing mechanisms are independent of each other. Then the digital output count is given by:

$$L(x) = \frac{CA(1+K)E(x)/E_r}{1+KE(x)/E_r} \quad (11)$$

where A is the scaling constant. If E_r is adjusted to $E(xf)$, the full-scale digital output is $L(xf) = AC$. Then:

$$L(x) = \frac{L(xf)(1+K)E(x)/E_r}{1+KE(x)/E_r} \quad (12)$$

The block diagram representation of the relevant circuit is given in Figure 2 of [12]. The proposed circuit's linearity of multi range sensors has been simulated with the virtual process having a temperature variation from 0°C to 100°C and the corresponding flowchart is shown in Figure 4.

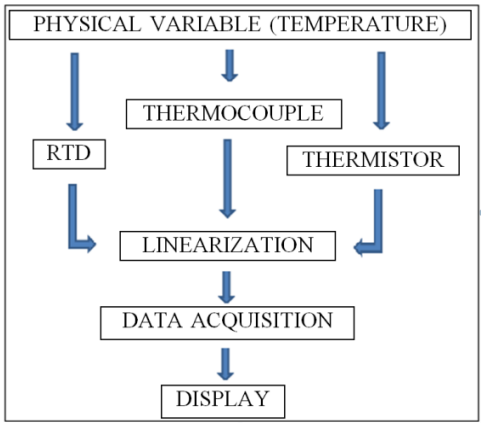

Fig. 4. Flowchart of the multi-range sensor system.

A simulation of the proposed circuit characteristic was conducted in LabVIEW [10]. For the linear NTC thermistor, the given parameters were V_{in} = 3.3V, R_1= 100Ω and B = 3000. The simulated thermocouple had a linear relation between temperature and output voltage, in a temperature range from 0°C to 60°C. For the third sensor, an RTD was used to measure the resistance change and output voltage with temperature with the following parameters: V_{in} = 5V, R_1 = R_2 = R_3 = 100Ω, R_{in} = R_f = 1000Ω, gain = 3.9 and V_{ref} = 5V.

H. Multi Range Temperature Sensor Simulation Block Diagram

The multi-range sensor system works through a varied range and employs multiple temperature sensors. Each sensor has a specific range to measure and to obtain value on the digital display and the corresponding sensor calculation. A simulation of the proposed characteristic was conducted with three linearized sensors (RTD, thermocouple, and thermistor). The diagram that integrates the graphic code of multi range sensor is shown in Figure 5.

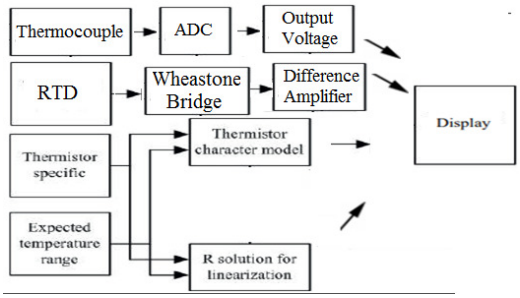

Fig. 5. Multi range temperature sensor simulation block diagram.

III. SIMULATION RESULTS

The NTC thermistor sensor was simulated for temperatures from 0°C to 60°C with the circuit shown in Figure 3. A good linear relation of the output voltage of the thermistor with temperature was acquired, as shown in Figure 6. The thermocouple sensor was simulated at the same range, with the circuit shown in [12]. A good linear relation of the output voltage with the temperature was acquired, as shown in Figure 7. For the RTD sensor, linearity was observed in the widest range (from 0°C to 850°C). After applying the feedback compensation method, it has been clearly improved as shown in Figure 8. The blue line graph is of the RTD sensor without linearity for the circuit diagram shown in Figure 1, and the orange line shows the obtained linearity of the RTD sensor for the circuit diagram shown in Figure 2.

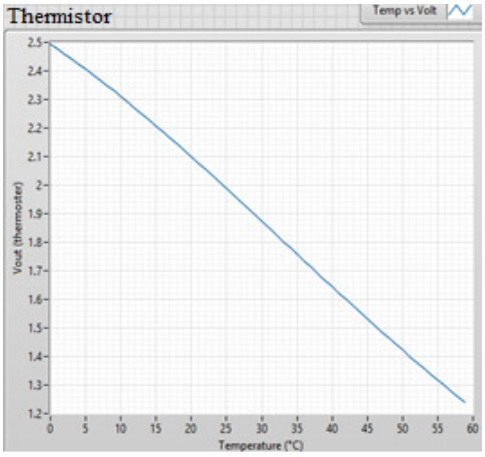

Fig. 6. Thermistor Voltage output vs input temperature.

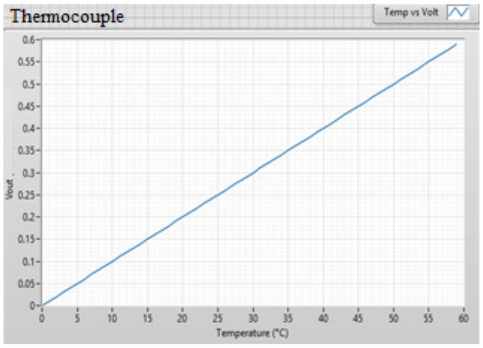

Fig. 7. Thermocouple Voltage output vs input temperature.

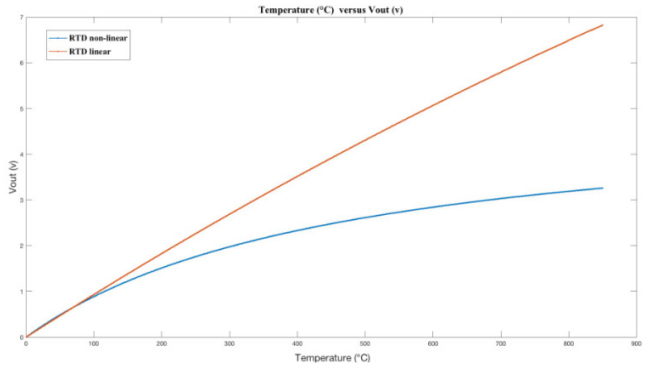

Fig. 8. RTD Voltage output vs input temperature

The proposed simulated system consists of three sensors (RTD, thermistor, and thermocouple). The ranges allocated to the RTD sensor, the thermistor, and the thermocouple were from 51°C to 60°C, from 41°C to 50°C, and from 31°C to 40°C respectively. The circuit and parameters for each sensor are the ones mentioned before, but with different ranges. This is an overall temperature measurement system which means that a temperature can be sensed by any sensor in the system as shown in Figure 9. The diagram that integrates the graphic code of multi range sensors is shown in Figure 10. When the temperature of the system is within the specified sensor range, the sensor starts to measure and shows that with a white LED for the measuring sensor and red LEDs for the sensors which are not measuring (Figure 9).

Fig. 9. Representation of measuring sensors with LEDs.

The multi range system provides a linear temperature with auto-selected response over a approximate temperature range from 0°C to +50°C for the thermistor, from 50°C to +70°C for the RTD, and from 70°C to +100°C for the thermocouple.

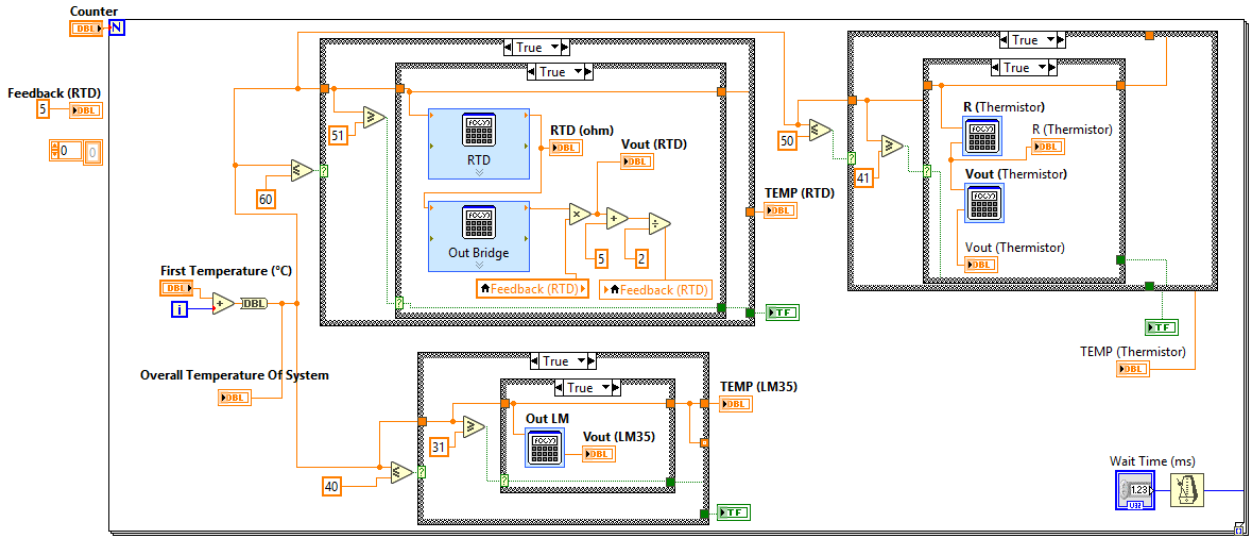

Fig. 10. Simulation of the multi-range temperature system.

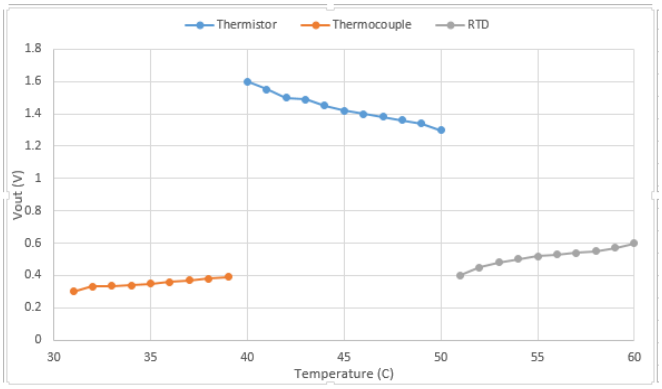

Fig. 11. The auto-selected temperature response of the proposed multi-range temperature measurement system.

A sufficient number of measurements were carried out by changing temperature ranges assigned to each sensor and the results were preserved. Thus, using the proposed method, the devised instrument can measure temperatures from a range of -50°C to around 1000°C.

IV. EXPERIMENTAL PART

In this part, we present the experimental results obtained with the developed multi range sensor (Figure 12). Three temperature ranges were selected for all sensors and the measurements were carried out with the proposed circuits as shown in Figures 2-3 and Figure 2 of [12] for the respective sensors, with the same parameters used in the simulations for each one. As seen in Figure 12, the obtained range of the corresponding output voltage for thermistor is from 1.41V to 1.65V, which corresponds to 41°C to 50°C. In this range, the thermistor is active (on). For the Thermocouple, the obtained range of the output voltage is from 1.41V to 1.65V, which corresponds to 41°C to 50°C. In this range, the thermocouple is active (on). Finally, for the RTD, the obtained range of the output voltage is from 1.41V to 1.65V, which corresponds to 41°C to 50°C. In this range, the RTD is active (on).

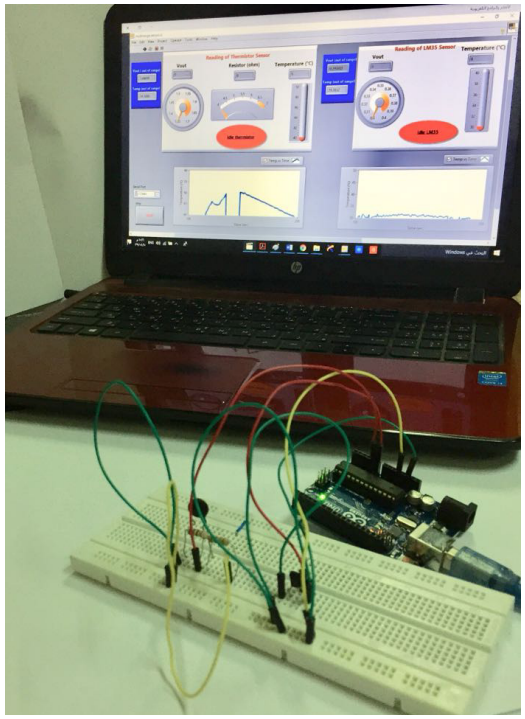

Fig. 12. Photo of the implemented and experimented upon multi-range temperature system.

V. CONCLUSION

As a part of our study of a wide-spectrum temperature measurement system with self-selected multi-sensor, we presented the design and testing of a high-precision wide-range sensor comprising of three different sensors (thermocouple, thermistor, RTD). A range was assigned to each sensor and simulations were performed in LabVIEW. The results from the carried out experiments were in good agreement with the simulation. This concept can be used for different applications such as MRI and ECT.

ACKNOWLEDGEMENT

This research was supported by the Deanship of Scientific Research, Imam Mohammad Ibn Saud Islamic University, Saudi Arabia, Grant No. 201314012.

REFERENCES

[1] P. Ramanathan Nagarajan, B. George, and V. J. Kumar, "A Linearizing Digitizer for Wheatstone Bridge Based Signal Conditioning of Resistive Sensors," *IEEE Sensors Journal*, vol. 17, no. 6, pp. 1696–1705, Mar. 2017, https://doi.org/10.1109/JSEN.2017.2653227.

[2] F. Reverter, J. Jordana, M. Gasulla, and R. Pallàs-Areny, "Accuracy and resolution of direct resistive sensor-to-microcontroller interfaces," *Sensors and Actuators A: Physical*, vol. 121, no. 1, pp. 78–87, May 2005, https://doi.org/10.1016/j.sna.2005.01.010.

[3] L. Guendouz, S. M. O. A. Ghaly, A. Hedjiedj, J. Escanyé, and D. Canet, "Improved Helmholtz-type magnetic resonance imaging coils with high-B1 homogeneity—Spherical and ellipsoidal four-coil systems," *Concepts in Magnetic Resonance Part B: Magnetic Resonance Engineering*, vol. 33B, no. 1, pp. 9–20, 2008, https://doi.org/10.1002/cmr.b.20106.

[4] A. Gani and M. J. E. Salami, "A LabVIEW based data acquisition system for vibration monitoring and analysis," in *Student Conference on Research and Development*, Jul. 2002, pp. 62–65, https://doi.org/10.1109/SCORED.2002.1033055.

[5] F. Alorifi, S. M. A. Ghaly, M. Y. Shalaby, M. A. Ali, and M. O. Khan, "Analysis and Detection of a Target Gas System Based on TDLAS & LabVIEW," *Engineering, Technology & Applied Science Research*, vol. 9, no. 3, pp. 4196–4199, Jun. 2019, https://doi.org/10.48084/etasr.2736.

[6] C. J. Kalkman, "LabVIEW: a software system for data acquisition, data analysis, and instrument control," *Journal of Clinical Monitoring*, vol. 11, no. 1, pp. 51–58, Jan. 1995, https://doi.org/10.1007/BF01627421.

[7] S. M. A. Ghaly, "LabVIEW Based Implementation of Resistive Temperature Detector Linearization Techniques," *Engineering, Technology & Applied Science Research*, vol. 9, no. 4, pp. 4530–4533, Aug. 2019, https://doi.org/10.48084/etasr.2894.

[8] S. M. A. Ghaly, K. A. Al-Snaie, M. O. Khan, M. Y. Shalaby, and M. T. Oraiqat, "Design and Simulation of an 8-Lead Electrical Capacitance Tomographic System for Flow Imaging," *Engineering, Technology & Applied Science Research*, vol. 11, no. 4, pp. 7430–7435, Aug. 2021, https://doi.org/10.48084/etasr.4122.

[9] S. M. A. Ghaly, K. A. Al-Snaie, and A. M. Ali, "Design and Modeling of a Radiofrequency Coil Derived from a Helmholtz Structure," *Engineering, Technology & Applied Science Research*, vol. 9, no. 2, pp. 4037–4043, Apr. 2019, https://doi.org/10.48084/etasr.2683.

[10] S. M. A. Ghaly, K. A. Al-Snaie, and O. K. Mohammad, "Spherical and Improved Helmholtz Coil with High B_1 Homogeneity for Magnetic Resonance Imaging," *American Journal of Applied Sciences*, vol. 13, no. 12, pp. 1413–1418, Dec. 2016, https://doi.org/10.3844/ajassp.2016.1413.1418.

[11] S. K. Sen, "An improved lead wire compensation technique for conventional two wire resistance temperature detectors (RTDs)," *Measurement*, vol. 39, no. 5, pp. 477–480, Jun. 2006, https://doi.org/10.1016/j.measurement.2006.01.002.

[12] A. A. Aly and A. S. A. El-Lail, "International Journal of Information Technology and Computer Science(IJITCS)," *International Journal of Information Technology and Computer Science*, vol. 5, no. 3, pp. 56–60.